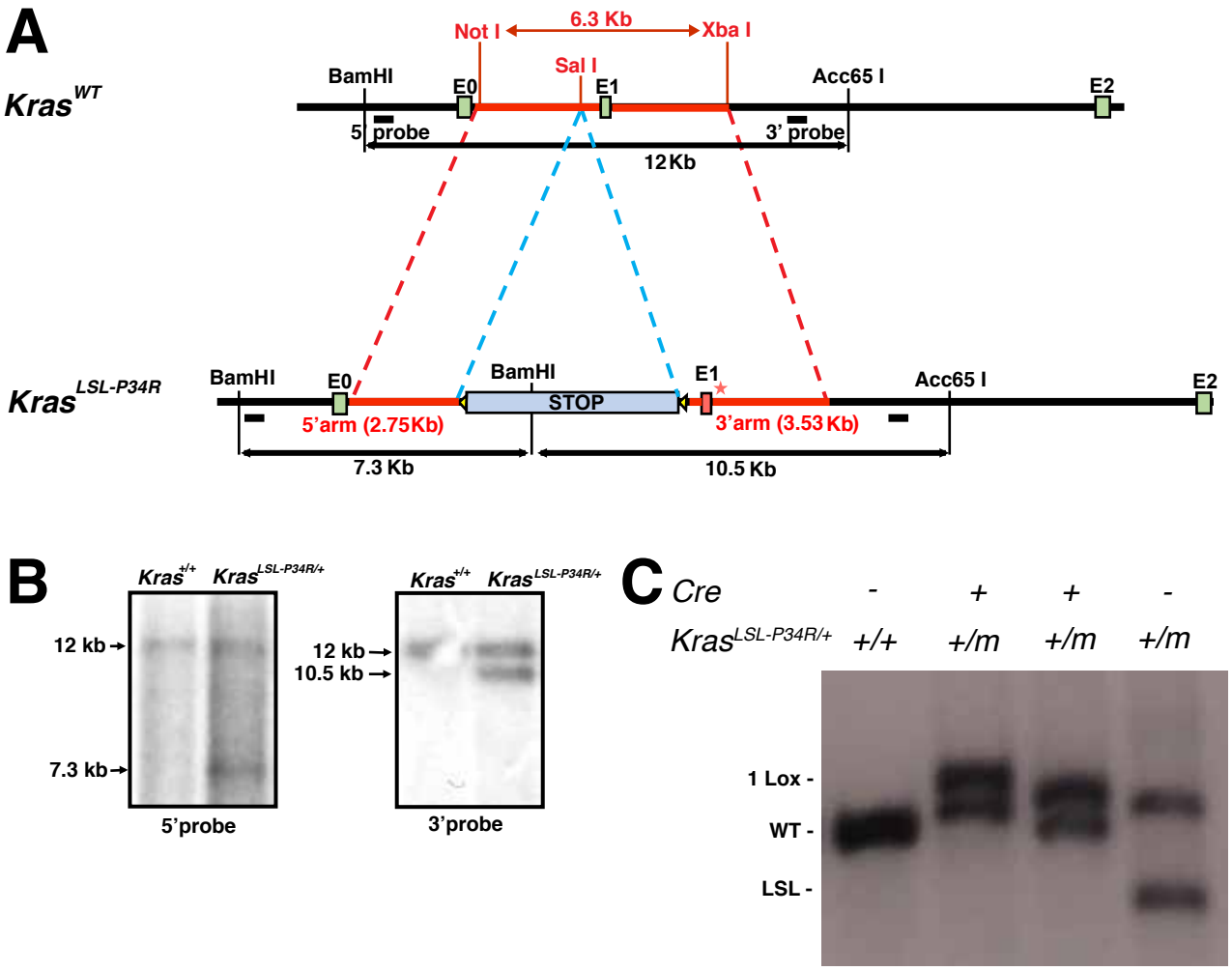

Supplemental Figure 1. Generation of the *Kras*$^{LSL-P34R/+}$ mice. (A) Schematic of the targeting strategy used to generate the *Kras*$^{LSL-P34R}$ allele. Red star represents the P34R mutation in Exon1. Targeting construct is shown in red. Yellow triangles represent *LoxP* sites flanking the transcriptional STOP cassette cloned upstream *Kras* Exon1. **(B)** Southern-blot indicating successful targeting and generation of *Kras*$^{LSL-P34R/+}$ mice. Probe location and expected DNA fragment mobilities are shown in **(A)**. **(C)** Gel analysis of PCR products amplified from the tail DNA of *CMV-Cre Kras*$^{LSL-P34R/+}$ neonates with fragments corresponding to the wild-type, non-targeted *Kras* allele (WT); the recombined targeted fragment (1 Lox) and the unrecombined targeted *LoxP-STOP-LoxP* allele (LSL).

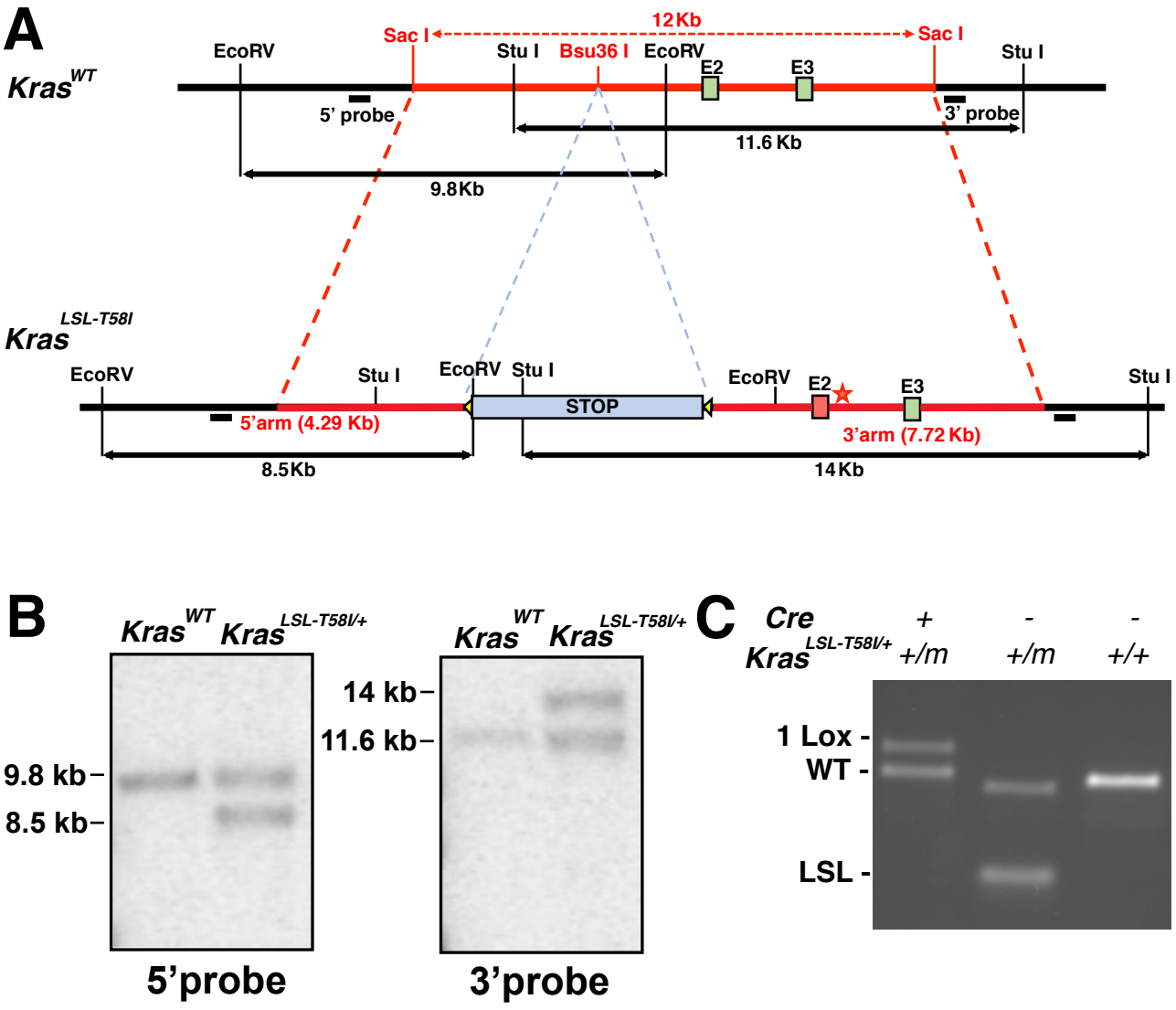

Supplemental Figure 2. Generation of the *Kras*$^{LSL\text{-}T58I/+}$ mice. (A) Schematic of the targeting strategy used to generate the *Kras*$^{LSL\text{-}T58I/+}$ allele. Red star represents the T58I mutation in Exon 2. Targeting construct is shown in red. Yellow triangles represent *loxP* sites flanking the transcriptional STOP cassette cloned upstream *Kras* Exon 2. **(B)** Southern-blot indicating successful targeting and generation of *Kras*$^{LSL\text{-}T58I/+}$ mice. Probe location and expected DNA fragment mobilities are shown in **(A)**. **(C)** Gel analysis of PCR products amplified from the tail DNA of *CMV-Cre Kras*$^{LSL\text{-}T58I/+}$ mice with fragments corresponding to the wild-type, non-targeted *Kras* allele (WT); the recombined targeted fragment (1 Lox) and the unrecombined targeted *LoxP*-STOP-*LoxP* allele (LSL).

A

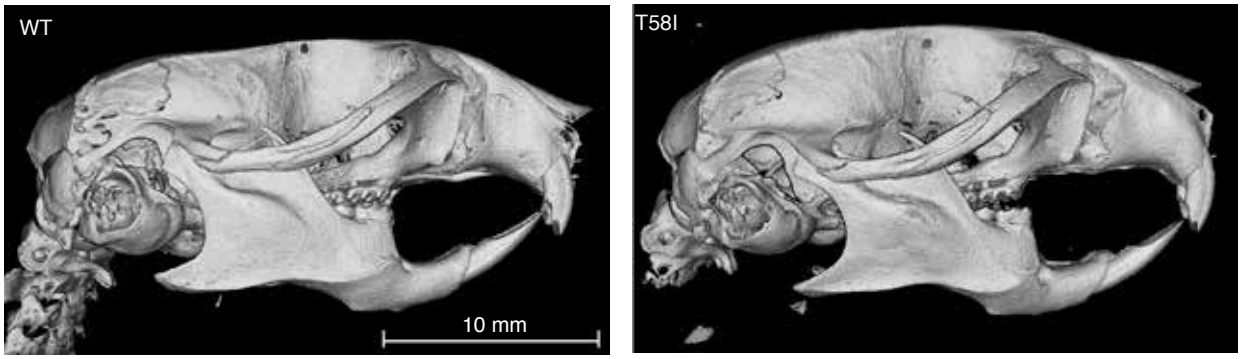

B

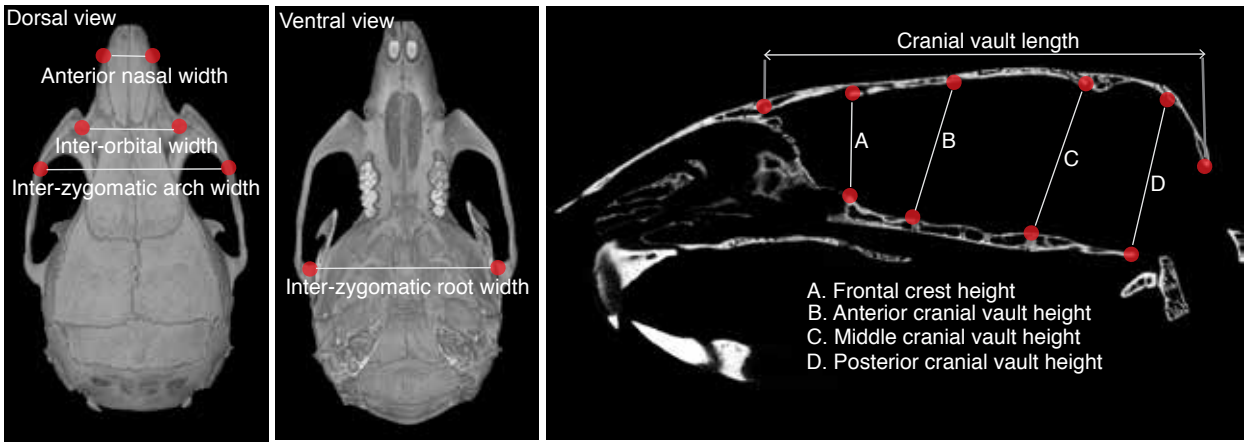

C

Measurements	*Kras*$^{+/+}$ (n=3)	*Kras*$^{+/T58I}$ (n=3)	*P value*
Anterior nasal width	2.74 ± 0.17	2.91 ± 0.04	0.17
Inter-orbital width	5.17 ± 0.08	5.46 ± 0.05	0.0045
Inter-zygomatic arch width	11.12 ± 0.13	11.71 ± 0.07	0.0021
Inter-zygomatic root width	10.60 ± 0.27	11.51 ± 0.14	0.0069
Cranial vault length	14.91 ± 0.46	15.74 ± 0.16	0.043
Frontal crest height	3.72 ± 0.55	4.41 ± 0.19	0.11
Anterior cranial vault height	5.06 ± 0.60	5.86 ± 0.38	0.12
Middle cranial vault height	5.82 ± 0.68	6.16 ± 0.59	0.55
Posterior cranial vault height	5.80 ± 0.79	5.95 ± 0.21	0.76

Supplemental Figure 3. Craniomorphometric analysis of the skull in *Kras*$^{T58I/+}$ mice. **(A)** 3D reconstructions of µCT scans showing the lateral aspect of 8-month old male WT and *Kras*$^{T58I/+}$ littermate mouse skulls (scale bar 10mm). **(B)** Schematics of the mouse skull depicting landmarks (red dots) used to obtain linear measurements. **(C)** Standard skull measurements in millimeters (mm) with standard deviations (SD) from microCT images of 8 months old male mice on a F1 B6/129 background. Measurements that are significantly different between WT and *Kras*$^{T58I/+}$ male mice by Student's t-test are shown in red font.

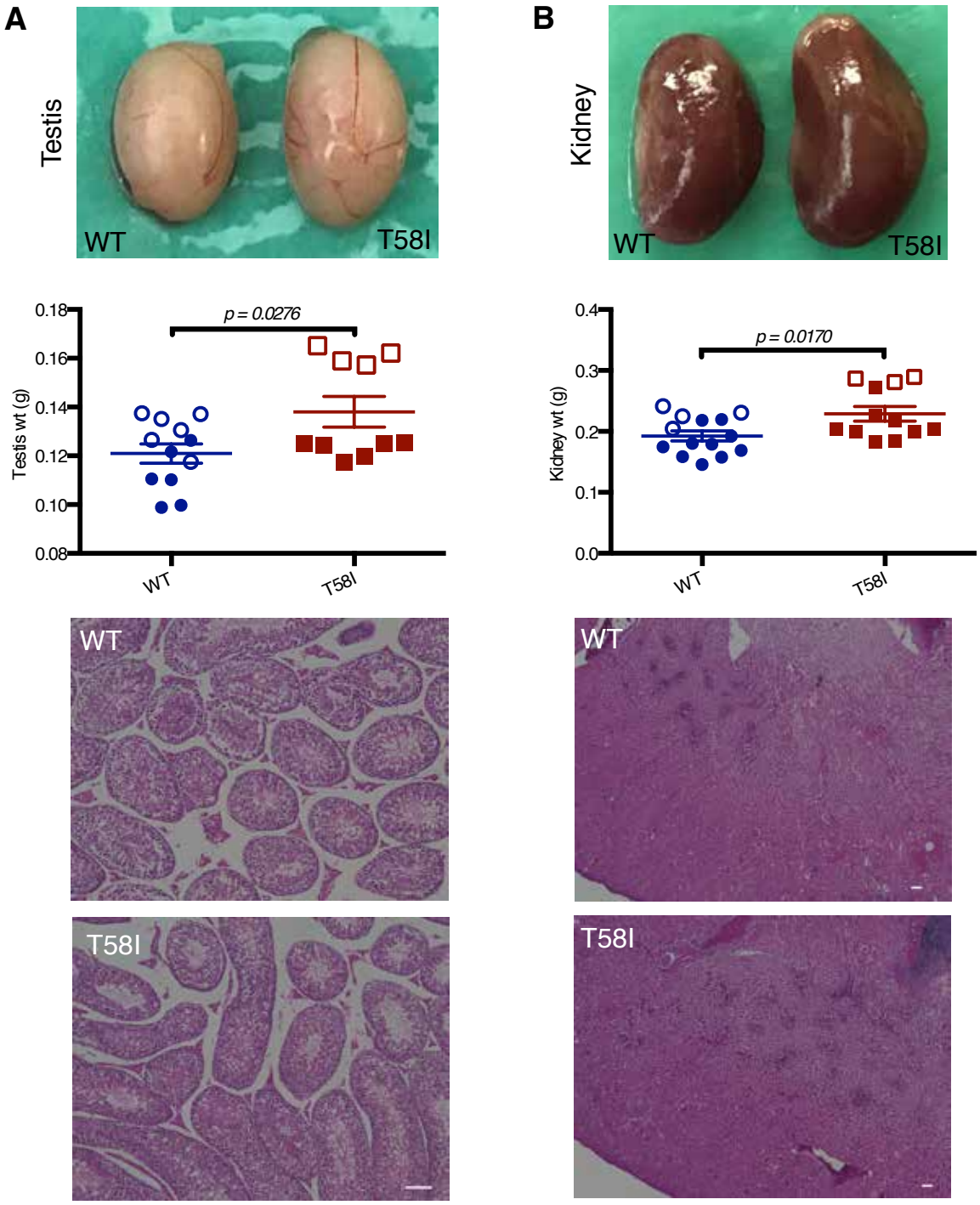

Supplemental Figure 4. Organ enlargement in 6 - 8 months old *Kras*$^{T58I/+}$ mice. Gross appearance (top), weights (mean and SEM are shown; center), and histologic appearance (bottom) of testes **(A)** and kidneys **(B)** from the WT and *Kras*$^{T58I/+}$ mice. Weight data were generated from both testes and from both kidneys for most animals. WT mice (n = 9, 7 males and 2 females) and their *Kras*$^{T58I/+}$ littermates (n = 8, 6 males and 2 females). The mice were on a F1 B6/129 (open circles or squares) or mixed B6/129 strain (closed circles or squares) background. Scale bar = 100µM. Statistical significance was evaluated by Student's t-test.

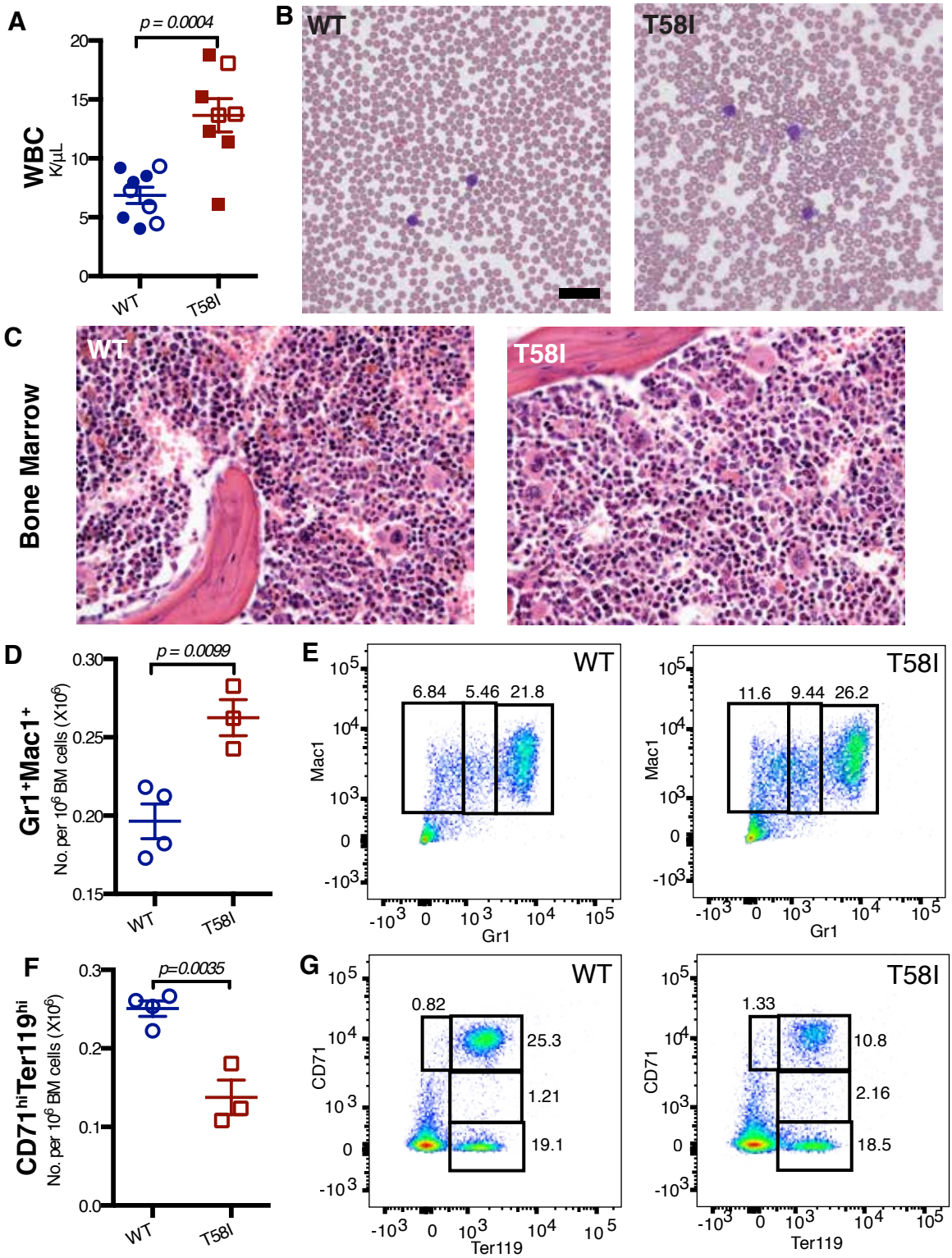

Supplemental Figure 5. Myeloproliferative disease in 6 - 8 month old *Kras$^{T58I/+}$* mice. (A) White blood counts (WBC) of wild-type (WT) mice (circles) and of their *Kras$^{T58I/+}$* (squares) littermates. **(B)** Representative Wright-Giemsa-stained blood from WT (left) and *Kras$^{T58I/+}$* (note increased polychromatophilic red blood cells, right) mice. Scale bar = 30µM. **(C)** Representative BM sections from WT (left) and *Kras$^{T58I/+}$* mice (right) stained with hematoxylin and eosin. Note decrease in BM erythroid precursors in *Kras$^{T58I/+}$* BM. **(D)** Frequency of BM neutrophils, which express both Gr1 and Mac1, in WT and *Kras$^{T58I/+}$* mice. **(E)** Representative flow cytometry plots showing an increase in the percentages of Mac1^{+} cells at all stages of differentiation in *Kras$^{T58I/+}$* mice, including Gr1^{hi} (mature neutrophils), Gr1^{lo} (immature neutrophils) and Gr1^{neg} (macrophages and monocytes) Mac1^{+} cells. **(F, G)** Frequency of BM basophilic erythroblasts (CD71^{hi}, Ter119^{hi}) in WT and *Kras$^{T58I/+}$* mice and representative flow cytometry plots. The mice used for these analyses were on a F1 B6/129 (open circles or squares) or mixed B6/129 strain (closed circles or squares) background. Student's t-test was used to assess the statistical significance of differences between WT and *Kras$^{T58I/+}$* mice.

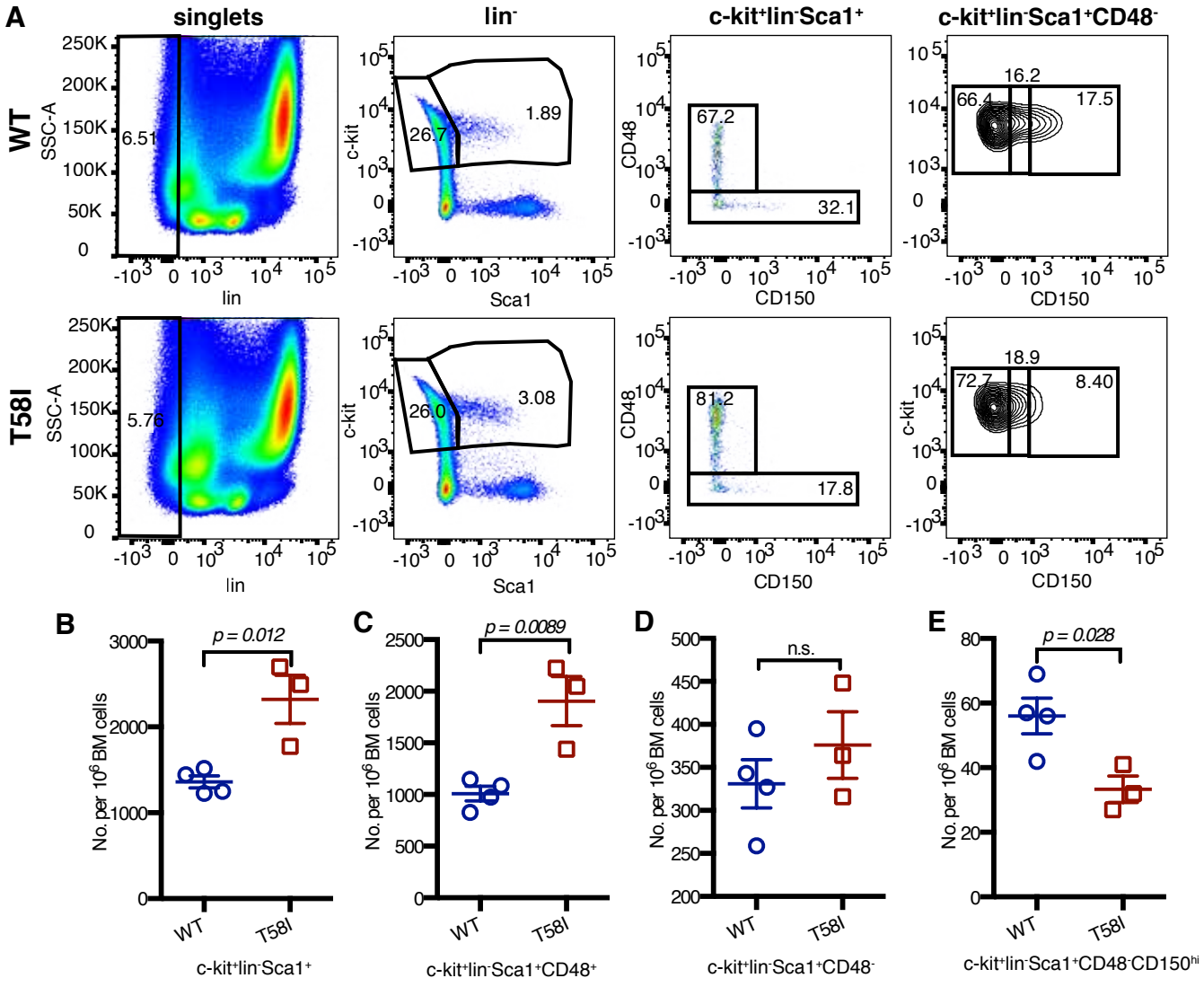

Supplemental Figure 6. Immunophenotypic analysis of bone marrow (BM) hematopoietic stem and progenitor cell populations for the mice shown in Supplemental Figure 5. (A) Representative flow cytometry plots showing the percentages of different subsets of gated cells in the BM of wild-type (top) and *Kras*$^{T58I/+}$ (bottom) littermates. **(B-E)** Frequencies of K$^+$L$^-$S$^+$ **(B)**, K$^+$L$^-$S$^+$, CD48$^+$ **(C)**, K$^+$L$^-$S$^+$, CD48$^-$ **(D)**, and K$^+$L$^-$S$^+$, CD48$^-$, CD150^{hi} **(E)** populations in mice of both genotypes. Student's t-test was used to assess the statistical significance of differences between WT and *Kras*$^{T58I/+}$ mice.

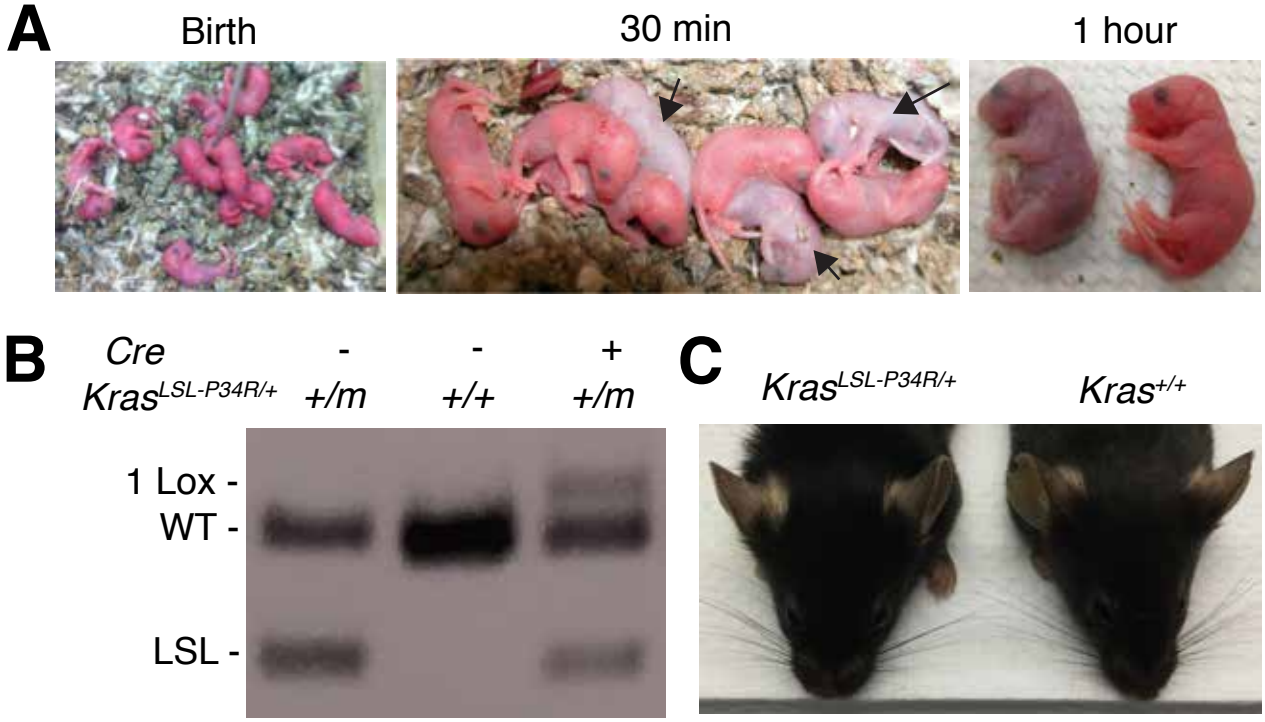

D

Patient #	*KRAS* mutation	Tissue sample(s): Type (proportion of mutant allele)
1	c.101C>G(p.Pro34Arg)	Leukocyte (44%)
2	c.101C>G(p.Pro34Arg)	Leukocyte (47%)
3	c.101C>G(p.Pro34Arg)	Leukocyte (42%) Fibroblasts from skin biopsy (47%)

Supplemental Figure 7. Early neonatal death of *CMV-Cre Kras$^{LSL-P34R/+}$* mice, mosaicism in a mouse that survived to adulthood, and analysis of *KRAS^{P34R}* patient DNA samples. (A) Representative photographs showing a normal pink appearance of neonatal mice generated by intercrossing *CMV-Cre* and *Kras$^{LSL-P34R/+}$* mice (left). Whereas wild-type (WT) and single mutant (*CMV-Cre Kras$^{+/+}$* or *Kras$^{LSL-P34R/+}$*) offspring remained well, *CMV-Cre Kras$^{LSL-P34R/+}$* offspring became cyanotic by 30 minutes after birth (black arrowheads; middle panel) and died by 1 hour of age (right). **(B)** Gel analysis of PCR products from tail DNA of *CMV-Cre Kras$^{LSL-P34R/+}$* mice showing amplification products corresponding to: (1) the wild-type, non-targeted *Kras* allele (WT); (2) the unrecombined targeted LSL allele; and, (3) the recombined targeted fragment (1 Lox) labeled. **(C)** Photograph of a mosaic *CMV-Cre Kras$^{LSL-P34R/+}$* mouse next to a WT littermate. **(D)** *KRAS* genotyping of blood leukocyte and/or fibroblast DNA from three children with heterozygous germline *KRAS^{P34R}* mutations at read depths of 1150-1600. Note that all of the samples are close to the expected 50:50 normal to mutant allelic ratio.

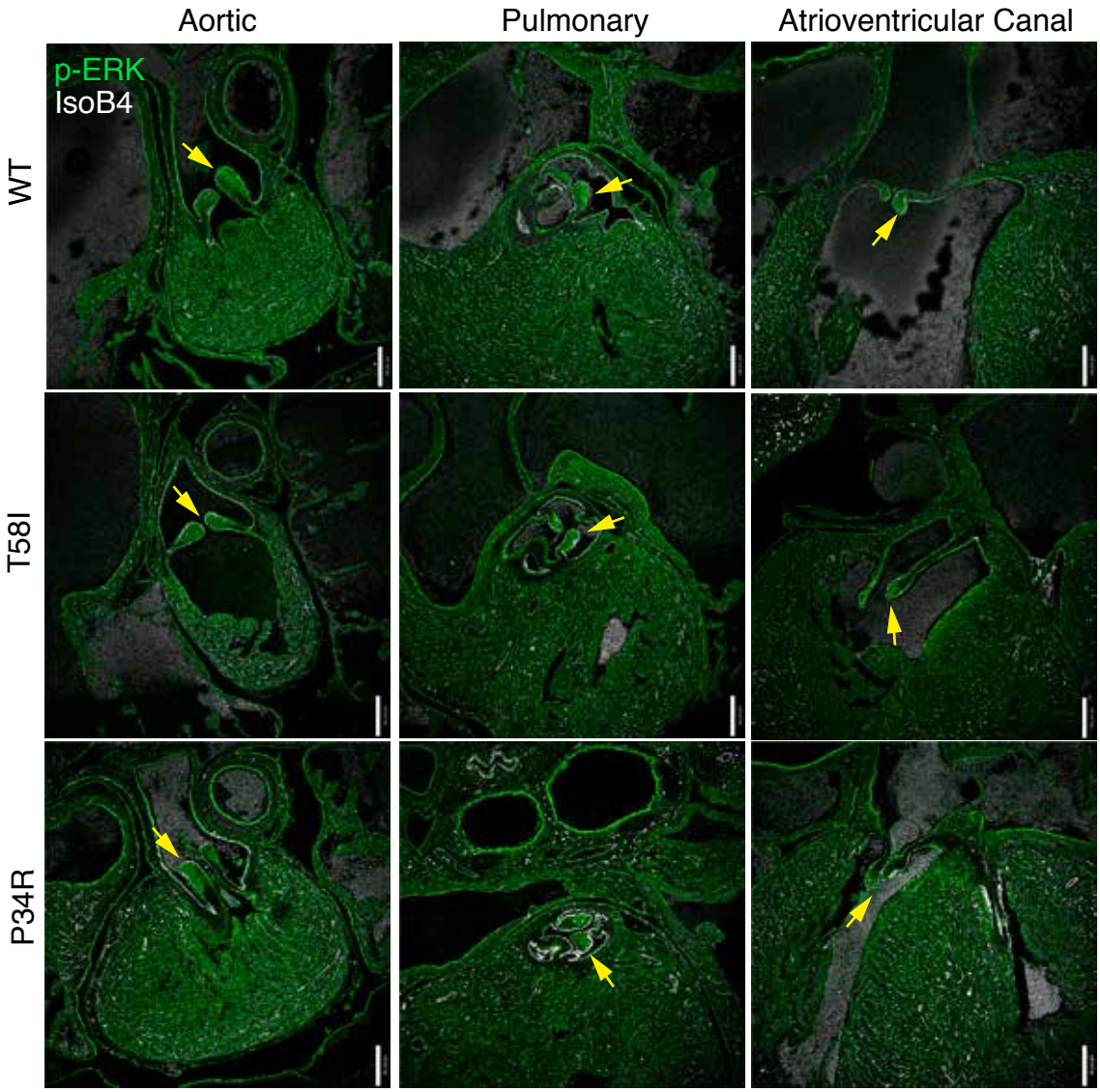

Supplemental Figure 8. Phospho-ERK staining of heart sections from wild-type (WT), *Kras*$^{T58I/+}$ (T58I), and *CMV-Cre Kras*$^{LSL-P34R/+}$ (P34R) newborn mice. Immunofluorescent microscopy images showing p-ERK (green) and the endothelial marker IsoB4 (white). Yellow arrows indicate the respective heart valves. Scale bars = 100μM.

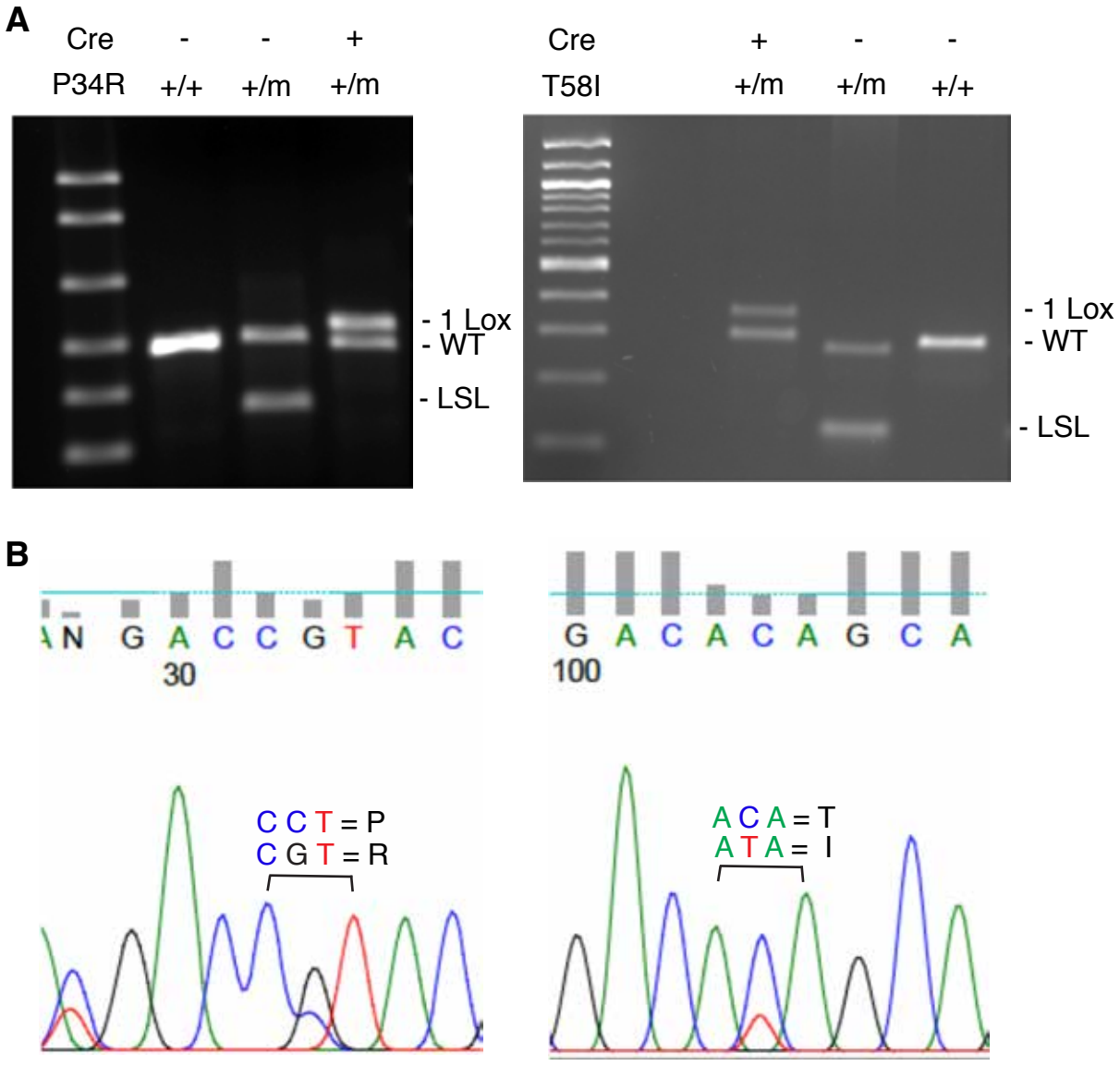

Supplemental Figure 9. Cre-recombination results in mutant transcript expression in the blood leukocytes of *Mx1-Cre Kras*$^{LSL\text{-}P34R/+}$ and *Mx1-Cre Kras*$^{LSL\text{-}T58I/+}$ mice. (A) Gel analysis of RT-PCR products amplified from the leukocytes of *Mx1-Cre Kras*$^{LSL\text{-}P34R/+}$ (left) and *Mx1-Cre Kras*$^{LSL\text{-}T58I/+}$ (right). PCR products generated from: (1) the wild-type, non-targeted *Kras* allele (WT); (2) the unrecombined targeted *LoxP*-STOP-*LoxP* allele (LSL); and, (3) the recombined targeted fragment (1 Lox) labeled can be distinguished by size. **(B)** DNA sequencing of RT-PCR products confirmed the expression of mutant transcripts.

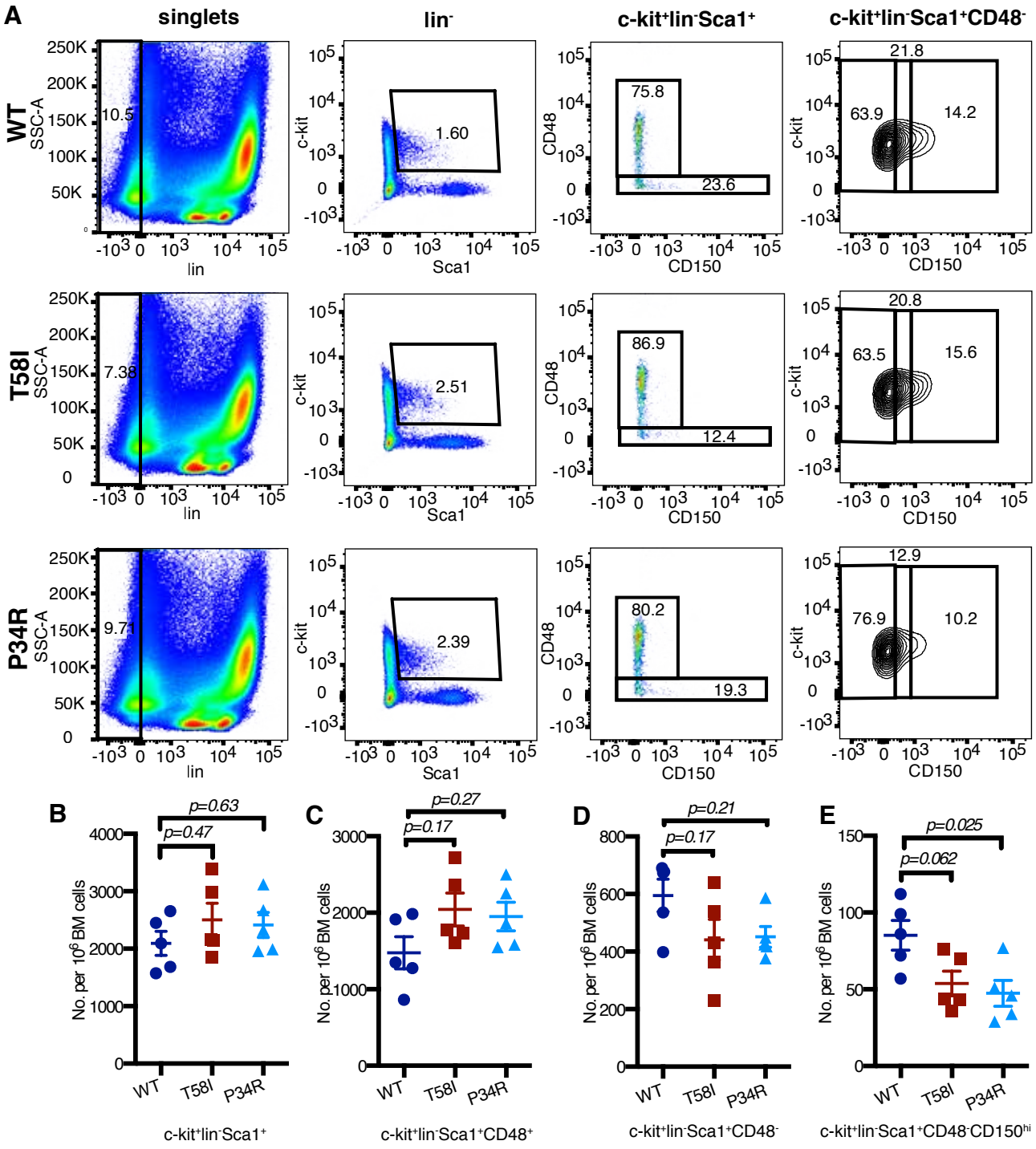

Supplemental Figure 10. Immunophenotypic analysis of hematopoietic stem and progenitor cell (HSPC) populations from old wild-type (WT), *Mx1-Cre Kras*$^{LSL\text{-}T58I/+}$, and *Mx1-Cre Kras*$^{LSL\text{-}P34R/+}$ mice. (A) Representative flow cytometry plots showing the percentage of different subsets of gated BM cells from each genotype. Frequencies of $K^+L^-S^+$ HSPC **(B)**; $K^+L^-S^+$, $CD48^+$ progenitor cells **(C)**; $K^+L^-S^+$, $CD48^-$ HSC; **(D)** and, $K^+L^-S^+$,$CD48^-$, $CD150^{hi}$ long-term HSC **(E)**. For this experiment, BM cells were collected from individual mice that were 19 (*Mx1-Cre Kras*$^{LSL\text{-}T58I/+}$) or 22 (WT and *Mx1-Cre Kras*$^{LSL\text{-}P34R/+}$) weeks old. Statistical significance was evaluated by ordinary one-way ANOVA with Tukey's multiple comparisons test.

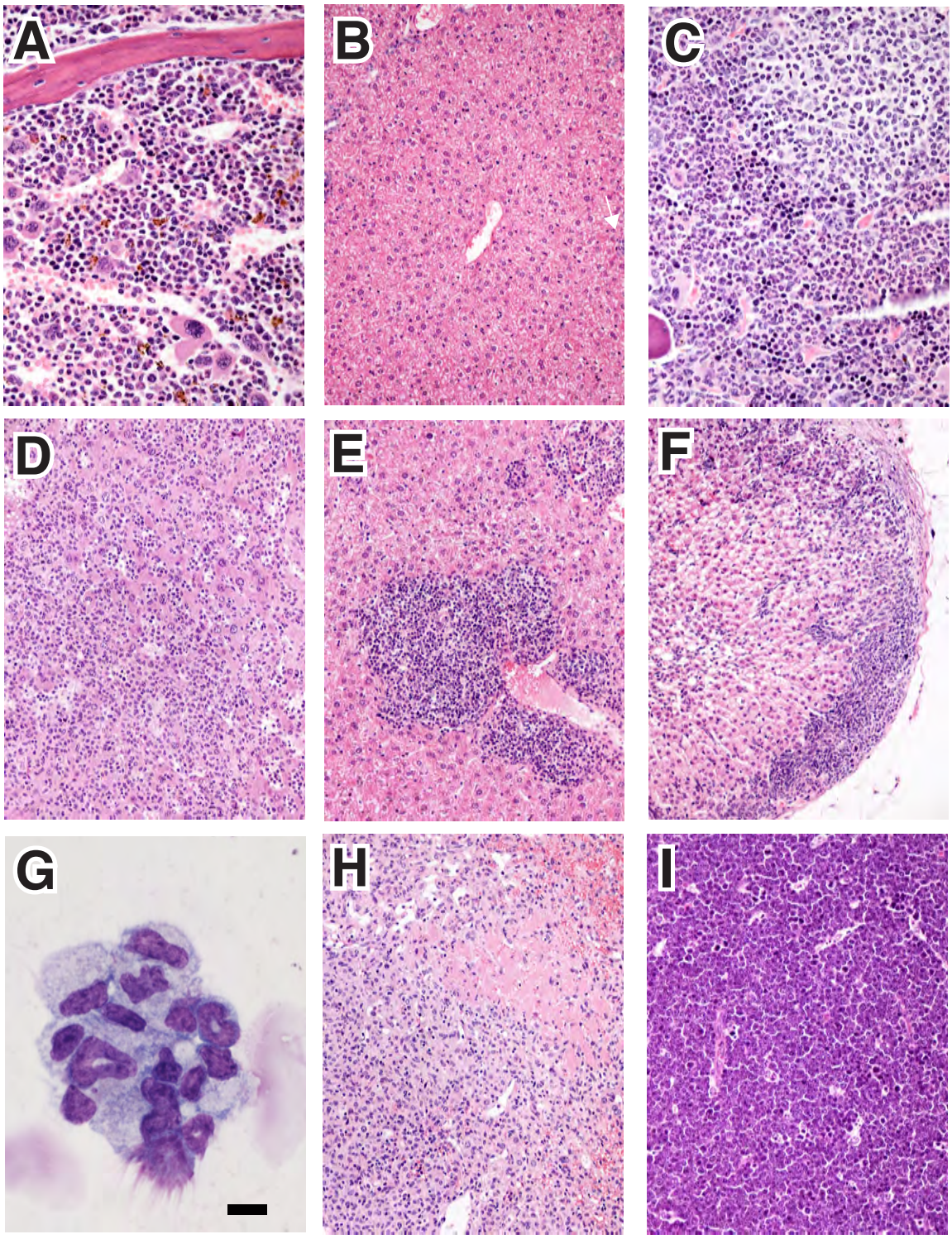

Supplemental Figure 11. Tissue sections from mice shown in Supplemental Table 5. (A, B) BM and liver sections of WT mouse 195; (**C**) Lymphohistiocytic lesions in the BM of T58I-mutant mouse 119; (**D**) Liver of T58I-mutant mouse 146 infiltrated with tumor cells suggestive of histiocytic sarcoma (**E, F**) Increased lymphocytes within the liver (**E**) and adrenal gland (**F**) from T58I-mutant mouse 194; (**G**) Abnormal BM cytospin from P34R-mutant mouse 161; (**H**) Liver of P34R-mutant mouse 161 infiltrated with tumor cells suggestive of histiocytic sarcoma (**I**) Enlarged lymph node from P34R-mutant mouse 285 with morphology consistent with lymphoblastic lymphoma. Scale bar = 30 μM (**A, C**), 60 μM (**B**, **D**, **E**, **F**, **H**, **I**), 8μM (**G**).

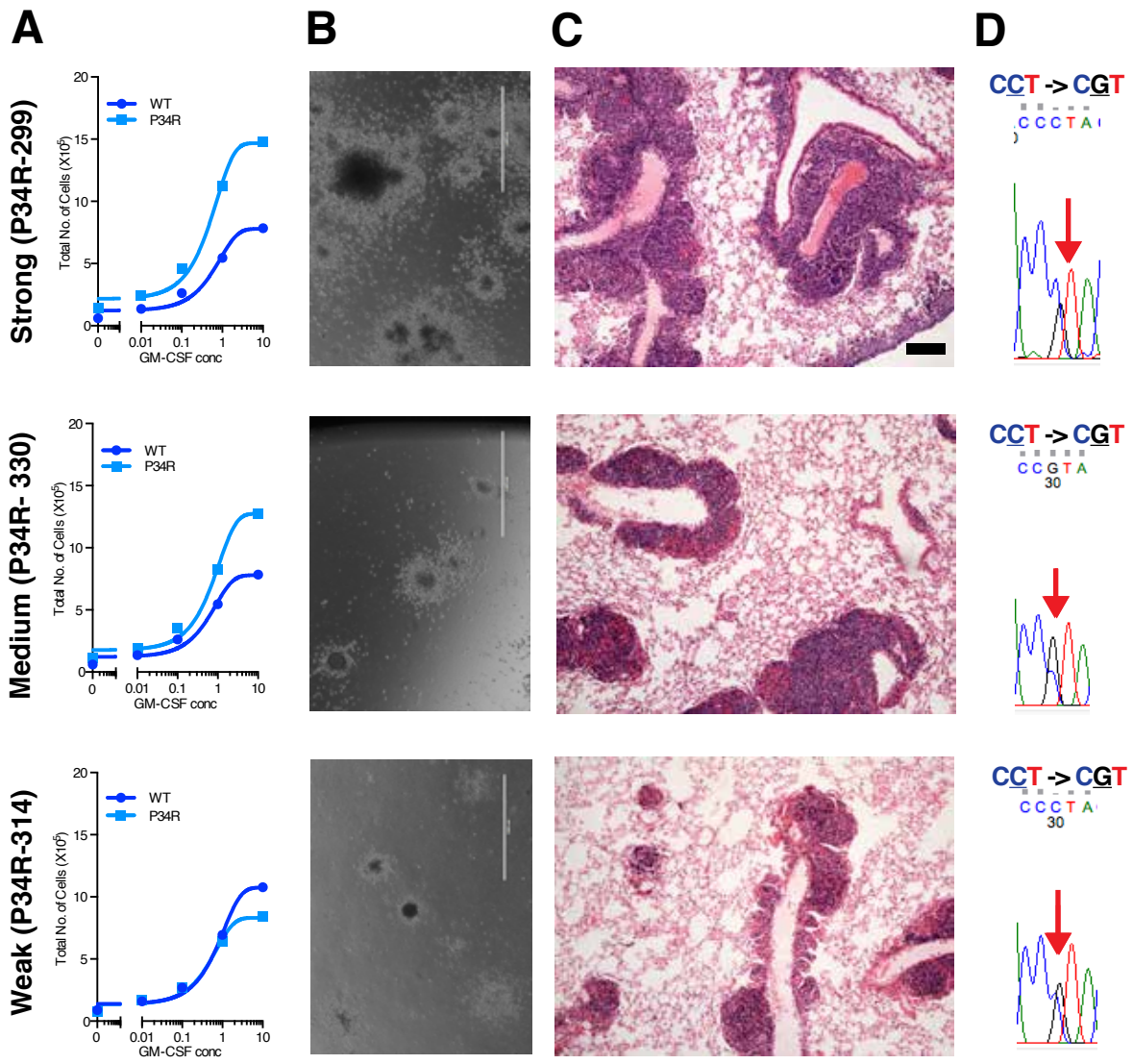

Supplemental Figure 12. Variable cytokine sensitivity and myeloid progenitor colony growth of bone marrow cells (BM) from *Mx1-Cre Kras*$^{LSL\text{-}P34R/+}$ mice with hematologic disease. (A) Proliferation of wild-type (WT) and *Mx1-Cre Kras*$^{LSL\text{-}P34R/+}$ c-kit^{+}, Mac1^{+} cells from individual mice in liquid cultures over a range of GM-CSF concentrations. **(B)** Representative cytokine-independent myeloid colonies grown from BM mononuclear cells. **(C)** Hematoxylin and eosin staining of lung sections; and, **(D)** DNA sequence chromatograms of BM DNA showing preservation of a near 50:50 wild-type to mutant ratio. Scale bar = 1000 μM for cytokine-independent colony assay and 120 μM for lung.

Supplemental Table 1
Effects of Strain Background on the Developmental Fitness of *Kras*$^{T58I/+}$ (T58I) Mice

C57BL/6J

Generation	WT male	WT female	T58I male	T58I female	Total male	Total female	Total WT	Total T58I	Total offspring
T58I* X C57 (BC1)	11	3	5	3	16	6	14	8 (36%)	22
T58I C57 (BC2)	14	8	2	2	16	10	22	4 (15%)	26
T58I C57 (BC3)	4	5	1	1	5	6	9	2 (18%)	11
Total	29	16	8	6	37	22	45	14	59
Percent	**49.2%**	**27.1%**	**13.5%**	**10.2%**	**62.7%**	**37.3%**	**76.3%**	**23.7%**	

129S4/SvJaeJ

Generation	WT male	WT female	T58I male	T58I female	Total male	Total female	Total WT	Total T58I	Total offspring
T58I* X 129S4 (BC1)	11	9	3	6	14	15	20	9 (31%)	29
T58I 129S4 (BC2)	3	3	2	2	5	5	6	4 (40%)	10
T58I 129S4 (BC3)	11	18	7	22	18	40	29	29 (50%)	58
Total	25	30	12	30	37	60	55	42	97
Percentage	**25.8%**	**30.9%**	**12.4%**	**30.9%**	**38.1%**	**61.9%**	**56.7%**	**43.3%**	

* The T58I (*Kras*$^{T58I/+}$) mouse was a hybrid F1 strain between C57BL/6J and 129S4/SvJaeJ. "BC" indicates the number of backcross generation. Deviation from the expected ratio of *Kras*$^{T58I/+}$ offspring when backcrossed to a C57BL/6J strain are highlighted in red text.

Supplemental Table 2

Blood cell values of 6–8 month old *Kras*$^{+/T58I}$ mice and their wild-type (WT) littermates on a 129S4XC57BL/6 mixed strain background

	WT (n = 9)	*Kras*$^{+/T58I}$ (n = 8)	P value
White Blood Cells			
Total Leukocytes (K/μL)	6.85 ± 1.79	13.66 ± 2.61	0.00043
Neutrophils	0.47 ± 0.23	1.01 ± 0.50	0.011
Lymphocytes	5.91 ± 1.79	11.51 ± 2.08	0.00074
Monocytes	0.29 ± 0.085	0.87 ± 0.27	7.58E-05
Eosinophils	0.14 ± 0.078	0.20 ± 0.21	0.43
Basophils	0.051 ± 0.033	0.066 ± 0.094	0.64
Red Cells and Platelets			
Red Blood Cells (M/μL)	9.61 ± 1.85	9.05 ± 0.57	0.43
Hemoglobin (g/dL)	15.3 ± 2.47	14.038 ± 0.88	0.22
Hematocrit (%)	51.86 ± 9.66	46.99 ± 3.91	0.23
MCV (fL)	54.1 ± 3.15	51.79 ± 2.35	0.18
RDW (%)	15.32 ± 0.47	18.2 ± 1.0	1.05E-05
Platelets (K/μL)	674.44 ± 274.23	856.75 ± 265.52	0.29

Values shown indicate the mean and (standard deviation) with parameters that are significantly different by Student's t-test shown in red font.

Supplemental Table 3

Blood cell counts in 9-24 week old *Mx1Cre Kras$^{LSL-T58I/+}$* and *Mx1Cre Kras$^{LSL-P34R/+}$* mice and their wild-type (WT) littermates

	WT (n=6)	*Mx1Cre Kras$^{LSL-T58I/+}$* (n=6)	*Mx1Cre Kras$^{LSL-P34R/+}$* (n=6)
White Blood Cells			
Total Leukocytes (K/μL)	9.58 (4.11)	11.00 (6.68)	10.51 (3.74)
Neutrophils	2.32 (1.66)	2.50 (2.58)	2.35 (1.41)
Lymphocytes	7.52 (4.87)	7.61 (4.56)	7.35 (2.63)
Monocytes	0.47 (0.32)	0.65 (0.49)	0.63 (0.36)
Eosinophils	0.20 (0.38)	0.19 (0.30)	0.13 (0.15)
Basophils	0.07 (0.12)	0.052 (0.085)	0.043 (0.061)
Red Cells and Platelets			
Red Blood Cells (M/μL)	8.56 (1.13)	8.78 (1.73)	8.75 (1.11)
Hemoglobin (g/dL)	13.1 (1.08)	12.45 (2.53)	13.18 (1.53)
Hematocrit (%)	43.15 (5.31)	41.23 (6.77)	45.35 (5.53)
MCV (fL)	50.52 (2.75)	47.27 (3.15)	51.93 (3.37)
RDW (%) 12.4-27.0	16.78 (0.42)	17.72 (0.48)*	17.13 (0.29)
PLT (K/μL)	775.5 (213.84)	896.5 (348.48)	922 (535.27)

Values shown indicate the mean and (standard deviation). Statistical significance was evaluated by one-way ANOVA. Values with statistically significant difference was denoted in red *p= ≤0.05.

Supplemental Table 4

Blood cell counts of sick 7-25 month old *Mx1Cre Kras$^{LSL\text{-}T58I/+}$* and *Mx1Cre Kras$^{LSL\text{-}P34R/+}$* mice and their healthy wild-type (WT) littermates

	WT (n=37)	*Mx1Cre Kras$^{LSL\text{-}T58I/+}$* (n=21)	*Mx1Cre Kras$^{LSL\text{-}P34R/+}$* (n=26)
Age at euthanasia (days)	16.45 (3.65)	15.79 (2.98)	15.47 (5.054)
White Blood Cells			
Total Leukocytes (K/μL)	6.69 (2.89)	11.52 (6.4)**	11.86 (6.13)**
Neutrophils	1.35 (1.27)	2.20 (1.59)	3.23 (4.36)*
Lymphocytes	4.76 (2.36)	7.82 (5.41)*	7.30 (3.55)*
Monocytes	0.38 (0.29)	1.18 (1.55)*	1.010 (1.14)
Eosinophils	0.16 (0.23)	0.24 (0.22)	0.26 (0.36)
Basophils	0.036 (0.044)	0.064 (0.070)	0.05 (0.063)
Red Cells and Platelets			
Red Blood Cells (M/μL)	8.96 (1.088)	8.24 (2.16)	7.83 (1.92)*
Hemoglobin (g/dL)	12.75 (1.62)	11.68 (2.30)	11.86 (2.82)
Hematocrit (%)	45.39 (4.24)	39.4 (8.08)*	39.77 (10.43)*
MCV (fL)	50.93 (3.66)	49.66 (11.86)	50.91 (5.27)
RDW (%)	17.31 (1.42)	18.37 (2.17)	18.76 (3.12)*
PLT (K/μL)	1044.90 (408.06)	976.5 (355.41)	935.92 (406.97)

The data are presented as mean and (standard deviation). Statistical significance was evaluated by one-way ANOVA. *p= ≤0.05, **p= ≤0.01 for mutant animals versus the WT controls.

Supplemental Table 5

Pathologic findings and disease classification in *Mx1Cre Kras$^{LSL-T58I/+}$* (T58I) and *Mx1Cre Kras$^{LSL-P34R/+}$* (P34R) mice with hematologic disease

Genotype	ID	Age (months)	Findings	Presumptive Diagnosis*
T58I	119	14.9	Lymphohistiocytic lesions in BM and spleen	Likely histiocytic Sarcoma
	127	17.6	Polychromatophilic erythrocytes visible on blood smear. Areas of lympho-histiocytic aggregates in BM and SP with splenomegaly, expanded red pulp and atypical expanded white. Liver with lesions suggestive of histiocytic sarcoma.	Possible histiocytic Sarcoma
	146	19.9	Liver infiltrated with tumor cells suggestive of histiocytic sarcoma, spleen has increased red pulp areas with what looks like histiocytic sarcoma	Histiocytic Sarcoma
	194	12.7	Increased lymphocytes around lung vasculature, in adrenal, and within the liver and spleen	Lymphoid proliferation (LP) or Lymphoma
P34R	161	19.9	Expansion of macrophages/lymphocytes in splenic white pulp, increased liver histiocytes.	Histiocytic Sarcoma
	197	17	Lympho-histiocytic aggregates, non-malignant thyroid adenoma in the neck.	Histiocytic Sarcoma, possibly with LP or Lymphoma
	208	26.6	Lymphohistiocytic tumor in liver, BM, spleen, lymphoid tissues, and lung	Histiocytic Sarcoma
	298	12.2	Lung lymphatics expanded and filled with lymphocytes as seen in human lymphoma	LP or Lymphoma
	256	20.9	Tumor in liver and in lung, BM mixed with small foci of tumor	Histiocytic sarcoma
	285	8.5	Enlarged thymus with morphology consistent with lymphoblastic lymphoma	Lymphoblastic lymphoma

All *Mx1Cre Kras$^{LSL-T58I/+}$* and *Mx1Cre Kras$^{LSL-P34R/+}$* mice required euthanasia for systemic hematologic disease. Abbreviations: BM = bone marrow; LP = lymphoid proliferation. *=Presumptive diagnoses were made based on gross and microscopic pathology; immunohistochemical staining and flow cytometry could not be performed for confirmation of cell lineages.

Supplemental Methods

Generation of *Kras^{P34R}* and *Kras^{T58I}* Mutant Mice. To generate the *Kras$^{LSL\text{-}P34R/+}$* strain, we cloned a 6.3Kb genomic fragment (129/Sv genetic background) harboring mouse *Kras* Exon 1 in pBluescript. Next, a Pro(CCT)-to-Arg(CGT) substitution at codon 34 was introduced by site-direct mutagenesis, using QuikChange II Site-Directed Mutagenesis Kit (Agilent Technologies Inc.). Finally, a LoxP-STOP-LoxP (LSL) cassette (50) was cloned upstream of *Exon 1^{P34R}*. To generate the *Kras$^{LSL\text{-}T58I/+}$* strain, we cloned a 12Kb genomic fragment (129/Sv genetic background) harboring mouse *Kras* Exon 2 in pBluescript. Next, a Thr(ACA)-to-Ile(ATA) substitution at codon 58 was introduced by site-direct mutagenesis, using QuikChange II Site-Directed Mutagenesis Kit (Agilent Technologies Inc.). Finally, a LoxP-STOP-LoxP (LSL) cassette (50) was cloned upstream of Exon 1^{T58I}.

TL1 ES cells (129/Sv genetic background) (51) were electroporated with the linearized pBluescript-LSL-Kras^{P34R} and pBluescript-LSL-Kras^{T58I} targeting constructs, and correctly targeted puromycin-resistant clones were identified by Southern blot. Two positive clones exhibiting a normal karyotype were used to generate chimeric mice by microinjection into B6 blastocysts. Chimeric mice were crossed to B6 females to obtain germline transmission of the *Kras$^{LSL\text{-}P34R}$* and *Kras$^{LSL\text{-}T58I}$* – targeted allele. Germline transmission of the targeted allele was confirmed by Southern blot analysis of tail DNA from the agouti offspring. Probes for southern blots were amplified by PCR from mouse genomic DNA using the following primers:

P34R(5')-Probe-F: 5'- TTC CTG CCT GAG TTG CAG CTT -3'
P34R-(5')-Probe-R: 5'- CTG TCT GCT GAA TAA TGA GCT CTT -3'
P34R(3')/T58I(5')-Probe-F: 5'- GGT AAG GAG AAC TGC AAA GA -3'
P34R(3')/T58I(5')-Probe-R: 5' – TGG CTG TGT ACT TTA AAA TG -3'
T58I(3')-Probe-F: 5' – TAT TCC TAG TAT ATA AAA GTG C -3'
T58I(3')-Probe-R: 5' – TCA AAC TAT AAC CCA TCT CAA G -3'

The resulting *Kras$^{LSL\text{-}P34R/+}$* and *Kras$^{LSL\text{-}T58I/+}$* mice were back-crossed for five generations to the C57BL/6J strain before crossing to *CMV-Cre* transgenic mice (JAX stock #006054) to eliminate the LSL cassette (15). Mice carrying the recombined *Kras$^{P34R/+}$* or *Kras$^{T58I/+}$* allele were identified by PCR genotyping. *Kras$^{T58I/+}$* mice were subsequently backcrossed to wildtype C57BL/6J (JAX stock #000664) or 129S4/SvJaeJ (JAX stock #009104) mice to eliminate the CMV-Cre transgene and to expand the lines. *Kras$^{LSL\text{-}P34R/+}$* and *Kras$^{LSL\text{-}T58I/+}$* in C57BL/6J were crossed to

Mx1-Cre transgenic mice on C57BL/6J strain background (JAX stock #003556)(26) to allow for tissue specific inducible expression of the P34R and T58I mutations. Male and female mice were used for experiments in equal genotypic ratios, and wildtype littermates were used as controls.

PCR Genotyping and pIpC Treatment. *Kras*^{P34R} alleles are genotyped with the following primers: WT for: 5'-ATG TCT TTC CCC AGC ACA GT -3', WT rev: 5'-TCC GAA TTC AGT GAC TAC AGA TG -3', LSL rev: 5'-CTA GCC ACC ATG GCT TGA GT -3'. The sizes of the diagnostic PCR products are 450bp for wildtype allele, 327bp for the unrecombined LSL allele, and 480bp for recombined 1-Lox allele. *Kras*^{T58I} alleles are genotyped with the following primers: WT for: 5'-GGA CTG TGC CTC ATC ACC AG -3', WT rev: 5'-GGA CTG TGC CTC ATC ACC AG -3' and LSL rev: 5'-CCA TGG CTT GAG TAA GTC TGC -3'. The sizes of the diagnostic PCR products are 256bp for wildtype allele, 122bp for the unrecombined LSL allele, and 309bp for recombined 1-Lox allele. Cre alleles are genotyped with Cre1: 5'-CTGCATTACCGGTCGATGCAAC-3' and Cre2: 5'-GCA TTG CTG TCA CTT GGT CGTG-3'. Presence of the Cre transgene give a 300bp product. Mice carrying the Mx1Cre transgene were injected intraperitoneally with 250 µg of polyinosinic-polycytidylic acid (pIpC) (Sigma-Aldrich) at 21 days of age. Leukocyte DNA was isolated using the GFX genomic blood purification kit (Amersham), and tissue DNA was isolated as described (52). cDNA was prepared from bone marrow cells using the RNeasy Mini Kit (Qiagen) followed by the SuperScript VILO Master Mix (Invitrogen). cDNA were amplified with the primers Kras 184-205 FOR 5'-GGA GAG AGG CCT GCT GAA AAT G-3' and Kras 426-406 REV 5'-CCA GTT CTC ATG TAC TGG TCC-3' primers. RT-PCR products were either treated with Exo-SAP-IT PCR Product Cleanup (Applied Biosystems) and directly sequenced with the primer Kras 241-262 5'- CGT AGG CAA GAG CGC CTT GAC G–3', or cloned into the pMiniT 2.0 vector using the NEB PCR cloning kit (New England Biolabs). Purified DNA plasmids were isolated from single colonies, and sequencing were performed using the SP6 Promoter or T7 Promoter primers.

Flow Cytometry. BM cells flushed from tibias and femurs were subjected to ammonium-chloride potassium red cell lysis before staining with antibodies. For identification of CD150^{hi}-HSC, CD150^{lo}-HSC, and CD150^{neg}-MPP, cells were pre-incubated with purified CD16/32 (2.4G2), followed by staining with a lineage cocktail of FITC-conjugated antibodies including B220 (RA3-6B2), CD8 (53-6.7), Gr-1 (RB6-8C5), CD3 (17A2), Ter119 (TER-119), as well as PE CD48 (HM48-1), BV510 Sca-1 (E13-161.7), and APC CD150 (TC15-12F12.2) from BioLegend

(San Diego, CA, United States) and APC780 c-kit (2B8) from eBioscience (San Diego, CA, United States).For identification of myeloid and erythroid cells, BM were stained with APC Mac-1, PacBlue Gr-1 (RB6-8C5), PECy7 Ter-119 (TER-119) and PE CD71. Stained BM cells were analyzed using a FACS LSRII instrument (Becton Dickinson, San Jose, CA, United States). FlowJo software (Tree Star, Inc., Ashland, OR, United States) was used to analyze and display the data. Cells were classified as $CD150^{hi}$-HSC, $CD150^{lo}$-HSC, or $CD150^{neg}$-MPP based in levels of CD150 expression.

KRAS Sequencing of RASopathy Patient DNA

Archival DNA samples from three unrelated RASopathy patients harboring the $KRAS^{P34R}$ mutation (c.101C>G) were reanalyzed by deep sequencing. All three individuals had been identified by previous diagnostic genetic testing performed after obtaining parental written informed consent in accordance with national regulations and additional consent was given for the use of remaining DNA samples for research purposes. One of three leukocyte DNA samples was from the index patient with this particular mutation reported by Schubbert et al. (7) The other two patients are unpublished cases, both with a clinical diagnosis of CFC syndrome. From one of them, DNA extracted from a skin fibroblast culture was available in addition to a standard blood leukocyte DNA sample. In order to determine precisely the variant allele frequency of $KRAS^{P34R}$ we used ultra-deep sequencing (mean coverage >1500x) of *KRAS* on the basis of a custom multi-gene panel (Nextera Rapid Capture Custom Enrichment Kit; Illumina, San Diego, CA), which is in routine use in the diagnostic laboratory at the University Hospital Magdeburg and covers all coding exons and flanking intronic sequence of ±20 nucleotides of the previously published RASopathy genes. Cluster generation and sequencing was performed on an Illumina MiSeq System (Illumina). Reads were aligned and mapped to the human assembly hg19 (GRCh37) using varvis 1.14.0 (Limbus Medical Technologies GmbH, Rostock, Germany). The number of reads showing the mutant nucleotide G were set in proportion to the number of reads with the C-allele (wildtype). A ratio (variant allele frequency) between 0.45 and 0.55 was considered as indication of a non-mosaic heterozygous status of the mutation in the respective tissue the DNA sample derived from.